HHS Public Access

Author manuscript

Nanomedicine. Author manuscript; available in PMC 2024 February 01.

Published in final edited form as:

Nanomedicine. 2023 February ; 48: 102642. doi:10.1016/j.nano.2022.102642.

Nipple fluid for breast cancer diagnosis using the nanopore of Phi29 DNA-packaging motor

Long Zhang, PhD[a,1], **Nicolas Burns, BS**[a,1], **Zhouxiang Ji, PhD**[a], **Steven Sun, PhD**[b], **Susan L. Deutscher, PhD**[c,*], **William E. Carson III, MD**[b,*], **Peixuan Guo, Ph.D.**[a,*] **[Director of Center for Nanobiotechnology and Nanomedicine]**

[a]Center for RNA Nanobiotechnology and Nanomedicine, College of Pharmacy, Dorothy M. Davis Heart and Lung Research Institute, James Comprehensive Cancer Center, College of Medicine, The Ohio State University, Columbus, OH 43210, USA

[b]OSU Comprehensive Cancer Center, The Ohio State University, Columbus, OH 43210, USA

[c]Department of Biochemistry, University of Missouri, Harry S. Truman Memorial VA Hospital, Columbia, MO 65211, USA

Abstract

Detection of cancer in its early stage is a challenging task for oncologists. Inflammatory breast cancer has symptoms that are similar to mastitis and can be mistaken for microbial infection. Currently, the differential diagnosis between mastitis and Inflammatory breast cancer via nipple aspirate fluid (NAF) is difficult. Here, we report a label-free and amplification-free detection platform using an engineered nanopore of the phi29 DNA-packaging motor with biomarker Galectin3 (GAL3), Thomsen-Friedenreich (TF) binding peptide as the probe fused at its C-terminus. The binding of the biomarker in NAF samples from breast cancer patients to the probe results in the connector's conformational change with a current blockage of 32 %. Utilization of dwell time, blockage ratio, and peak signature enable us to detect basal levels of biomarkers from patient NAF samples at the single-molecule level. This platform will allow for breast cancers to be resolved at an early stage with accuracy and thoroughness.

Keywords

Biomarker; Noninvasive; DNA-packaging motor; Nanopore sensing; Tumor diagnosis

[*]Corresponding authors at: The Ohio State University, Biomedical Research Tower, 460 W. 12th Avenue, Rm. 912, Columbus, OH 43210, USA. DeutscherS@missouri.edu (S.L. Deutscher), William.Carson@osumc.edu (W.E. Carson), guo.1091@osu.edu (P. Guo).
[1]These authors contributed equally.

CRediT authorship contribution statement

P.G. conceived and designed the project. L.Z. prepared the manuscript, L.Z., N.B., J.Z. and S.D carried out the experiments and analyzed the data. S.S. and W.C. collected the NAF samples and P.G. co-wrote the manuscript, and all authors refined the manuscript.

Declaration of competing interest

P.G. is the consultant and licensor of Oxford Nanopore Technologies; the cofounder of Shenzhen P&Z Bio-medical Co. Ltd., as well as the cofounder and the chairman of the board of ExonanoRNA, LLC.

Breast cancer is one of the leading causes of death among women around the world. It is generally asymptomatic at the early stages. Current screening tools such as mammography and breast examination miss up to 40 % of early-stage breast cancers and are ineffective in detecting cancer in young women[1]. Some breast tumors might have already metastasized by the time a mass is detectable. To reduce morbidity and mortality, more sensitive methods for the early diagnosis of breast cancer are desirable. The cancer secretome (secreted antigens and metabolites) represents a very promising set of cancer-related biomarkers that can be derived from body fluids mirroring the tissue-specific tumor microenvironment. The breasts of adult non-lactating women secrete a small volume of fluid, called “nipple aspirate fluid” (NAF), into the breast ducts[2]. NAF has been used for the diagnosis and risk assessment for a variety of diseases such as bacterial infection, viral infection[3]. Collection of nipple fluid, which is secreted by non-pregnant women, is one method of acquiring diagnostic samples for breast cancer[4-7]. However, inflammatory breast cancer is often confused with mastitis, an infection of the breast. This is because the symptoms of inflammatory breast cancer are very similar to mastitis. Currently, differential diagnosis between inflammatory breast cancer and mastitis via nipple aspirate fluid is also challenging. The NAF secreted by epithelial and stromal cells lining the breast duct can be noninvasively collected from patients using breast pumps. With its abundant supply of candidate biomarkers, the NAF secretome represents an excellent opportunity for early diagnosis of breast cancer, limiting the decreased tumor-specificity of surrogate breast cancer biomarkers circulating in the blood[1,8,9]. The Thomsen–Friedenreich antigen (TF; CD176, Galβ1-3GalNAcα-) is a tumor-specific carbohydrate antigen and a promising therapeutic target. The TF antigen has a high prevalence in many types of carcinoma, is involved in metastasis and potentially plays a role in immunosurveillance and therapy[10]. GAL3 is a β-galactoside-binding protein that has been found to be involved in tumor cell growth, anti-apoptosis, adhesion, angiogenesis, invasion, and distant metastases[11,12]. TF antigen and GAL3 antigen are secreted preferentially in nipple aspirate fluid from breast cancer patients[13-19]. It is reported that the concentration of the TF antigen in noncancer NAF is almost undetectable. In the breast cancer NAF samples, the median concentration of TF antigen was 480 ng/μl (range, 0–2240 ng/μl)[14]. Detection of basal levels of biomarkers from patient NAF samples in the presence of many contaminants requires a high-sensitivity platform.

Detection of secreted proteins is a powerful method for analyzing changes in global expression patterns as a function of physiological and disease processe[9,13,14,20,21]. Common methods for proteomic profiling include: 2D gel electrophoresis[20]; Mass spectrometry (MS) based MALDI (Matrix-Assisted Laser Desorption Ionization) [22-24]; and, 1D and 2D Liquid Chromatography (LC) coupled with UV or MALDI detection[22,25,26]. Each technique has distinct advantages and disadvantages, relating to low threshold and specificity of detection, dynamic range, multiplexing capability, precision, throughput, and ease of use[27,28].

Nanopore-based single-molecule detection has been used for the sensing of a myriad of biomedical macromolecules[29-32]. The ingenious design of the bacterial virus phi29 DNA-packaging motor with its elegant channel has inspired its application in nanotechnology. The central hub of the phi29 motor is a connector composed of 12 identical GP10 proteins, which encircle to form a dodecameric channel for dsDNA translocation. The funnel-shaped connector's pore is 3.6 nm in diameter at the narrow end and 6 nm at its wider end[33,34].

The phi29 motor channel has been successfully inserted into the planar lipid bilayer to serve as a nanopore for real-time detection of analytes at the single-molecule level[6,32,35-38]. The connector shrinks and exhibits discrete step-wise conformational changes in response to ligand binding to its C-terminal end[39,40]. The three steps of gate size transition has inspired the application of the functionalized phi29 connector with various probes for single-molecule detection of antigens[39].

In this study, we developed the phi29 connector for detecting breast cancer biomarkers from clinical NAF samples with high sensitivity (single molecule detection) and specificity (detection in the presence of contaminants). We found GAL3 or TF binding peptide modified connectors can specifically bind to the appropriate biomarkers but will not with a control protein (negative sample). We found the NAF samples from breast cancer patients but not healthy ones could specifically bind to the modified nanopores and produce an observable signal to correlate. Utilizing dwell time, blockage ratio, and signature shape have enabled us to detect the specific binding events at the single-molecule level. Our platform has shown great promise for the detection and validation of biomarkers from complex clinical samples.

Materials and method

Materials

The phospholipid 1,2-diphytanoyl-sn-glycerol-3-phosphocholine (DPhPC) was purchased from Avanti Polar Lipids, Inc. Organic solvents (n-decane, hexane and chloroform) were obtained from Fisher Scientific, Inc. and TEDIA, Inc., respectively. The human Galectin-3 protein were purchased from Abcam. Free TF and TF-HSA (TF antigen was conjugated to human serum albumin) were purchased from Dextra Laboratories. The control protein (Carbonic Anhydrase from bovine erythrocytes, 29 kDa) was purchased from Thermo Fisher Scientific. All other reagents, if not specified, were purchased from Fisher Scientific.

Cloning, expression and purification of mutant Phi29 channels with TF and GAL3 probe

The expression and purification of phi29 N-His-GP10-GAL3 and N-His-GP10-TF probes was reported previously[39,41]. For cloning of the engineered Phi29 connector channel, the recombinant plasmids were constructed by introducing a GAL3 probe (ANTPCGPYTHDCPVKR) or TF probe (IVWHRWYAW-SPASRI) to the C-terminus of the connector; a His-tag was inserted into the N-terminal for purification and followed by a GGENLYFQG sequence. To increase the flexibility, a GG linker was added between the ORF and probe.

The connector mutants constructed were expressed and then purified with nickel affinity chromatography. Cells were resuspended with His Binding Buffer (Tris-HCl 0.1 M, NaCl 0.5 M, ATP 50 μM, Glycerol 14.4%, Imidazole 5 mM), and the cleared lysate was loaded onto a HisBind Resin Column (Novagen) and washed with His Washing Buffer (Tris-HCl 0.1 M, NaCl 0.5 M, ATP 50 μM, Glycerol 14.4 %, Imidazole 50 mM). The C-terminal Histagged connector was eluted by His Elution Buffer (Tris-HCl 0.1 M, NaCl 0.5 M, ATP 50 μM, Glycerol 14.4 %, Imidazole 1 M).

Enzyme linked immunosorbant assay

To test the TF binding to TF motor, the TF enzyme linked immunosorbant assay was performed. Asialoglycophorin, glycophorin, asialofetuin or no protein coated on a plate o/n at 4C°. Plates were blocked 2 h in 6%BSA/TBS washed and incubated for 2 h in motor or biotinylated PNA (BPNA) in 1% BSA/ATP/TBST, washed and incubated in appropriate secondary antibody for 1 h at RT, washed and developed. Plates were read at 405 nm.

GAL3 enzyme linked immunosorbant assay was used to evaluate the binding efficiency of GAL3 protein to GAL3 motor. GAL3 (0.25 μg/well) was coated on a plate overnight at 4 °C in carbonate buffer and blocked 2 h at RT in 6 % BSA/TBS. Various concentrations of biotinylated peptide, motor or anti-GAL3 antibody were added to well and incubated for 2 h in 1% BSA/ATP/TBST. The wells were washed and appropriate secondary antibody was incubated 1 h at RT (SA-HRP, anti-HisAb-HRP or antiRat-HRP), wells washed and developed. Plates were read at 405 nm. Background binding to no protein wells was subtracted out. The secondary antibodies used in this study are 6xHis mAb-HRP Conjugate, Clonetech (Cat:631210, Takara Bio). goat anti-rat IgG-HRP (sc-2006, Santa Cruz Biotechnology, Inc).

Incorporation of connector into liposomes

The incorporation process contains dehydration and hydration steps[42]. Connector-reconstituted liposomes were prepared using a dehydration rehydration method. Briefly, 100 μl 10 mg/ml DPhPC in chloroform was dried for 4 min, under a vacuum by the evaporator (Buchi). The connector (final concentration 500 μg/ml) and liposome buffer (Liposome buffer: 3 M KCl, 250 mM sucrose, 5 mM HEPES, pH 7.4) were added and vortexed thoroughly to form giant unilamellar vesicles (GUVs). To prepare homogenous proteoliposomes, the GUVs were then filtered through a 0.4 μm polycarbonate membrane for around 25–30 times using the extruder (AvantiPolar Lipids).

Electrophysiological assays

The lipid bilayer membrane was formed on the Teflon partition membrane by pre-painting both sides of the Teflon partition (pore size: 200 μm) with lipid solution A. After that, both compartments in the black lipid membranes (BLM) chamber were filled with a conducting buffer (0.15 M KCl, 5 mM Tris, pH 7.4, if not specified) and then pipetted 0.5 μl of lipid solution B into the aperture to form the lipid bilayer. A pair of Ag/AgCl electrodes were placed in both chambers. All the proteins (1 mg/ml) were added to both chambers. The current trace was recorded by Bilayer Clamp Amplifier BC535 (Warner Instruments) system with an Axon DigiData 1440 A analog-digital converter (Molecular Devices). To test the clinical samples, NAF concentration was measured (TF 480 ng/ul)[14] and diluted ten times with PBS. After that, the same volume of health and breast cancer NAF samples was used and added to both chambers to test the binding on the corresponding channels. Data were recorded at 1 K Hz bandwidth with a sampling frequency 20 KHz. The Clampex 10 (Molecular Devices), Clampfit 10 (Molecular Devices), MOSAIC and PRISM were used to collect and analyze data.

Collection of nipple aspirate fluid

This collection of NAF samples was conducted under the auspices of The Ohio State University Comprehensive Cancer Center (OSUCCC) and approvaled by Cancer Institutional Review Board (IRB) (Approval No. OSU-16288). NAF from both breasts of the 3 subjects, two breast cancer positive and one negative, was collected using a published technique[5,20,43]. Briefly, before aspiration was attempted, the nipple was cleansed with an alcohol wipe. A small amount of lotion was be placed on the breast and the breast was gently massaged from the chest wall towards the nipple for 1 min. A nipple aspiration device was used to collect the sample. The fluid droplets were collected into capillary tubes. The extracted samples were processed and stored at −80 °C and batched for analysis. The detailed patient parameters are described in Table 1.

Statistical analysis of data

Data was collected via counting of peaks occurring within a set period and the percentage of blockage. Blockages of ~32 % of the original voltage were considered events and those with a dwell time exceeding 50mS were considered to be specific binding. Permanent binding events were counted as well. Data were collected in triplicate from separate experiments then averaged to obtain values for non-specific, specific, and permanent binding events.

Results

Incorporation of the breast cancer biomarker binding peptide to the C-terminal end of the connector

Two reengineered phi29 connector channels were constructed with GAL3 or TF antigen binding peptides at their C-terminus. The GAL3 and TF antigen binding peptide engineered phi29 connectors were incorporated into planar lipid membranes to form a membrane-embedded nanopore, as previously described (Fig. 1A)[39]. The GP10 ORF with 6His tag at its N-terminus and a GAL3 binding peptide (ANTPCGPYTHDCPVKR) or TF binding peptide (IVWHRWYAWSPASRI) at the C-terminal end was inserted into pET-21a prokaryotic expression vector. Therefore either the GAL3 or TF binding peptides can be located at the C-terminal. To provide end flexibility, a linker with 2 glycines was included between the GP10 ORF and the binding peptide probe (Fig. 1B, C). The reengineered connectors before and after purification were identified by a 10 % SDS-PAGE gel (Fig. 1D). The molecular weights of N-His-GP10-GAL3 and N-His-GP10-TF recombinant connector subunits were similar at about 38 kDa.

Evaluation of biomarkers binding to the channel by Enzyme Linked Immunosorbant Assay (ELISA)

The binding efficiency of breast cancer biomarkers TF and GAL3 was firstly evaluated by ELISA, as previously descrised[44-46]. Asialoglycophorin (TF), asialofetuin (ASF, another TF molecule) and glycophorin or no protein coated on a plate. After that EpCAM (negative control channel) or TF channel were added and biotinylated peanut agglutinin (PNA) as the positive control. The ELISA results suggested that TF can only bind to TF channel with an increased absorbance at OD405 nm but not the EpCAM channel (Fig. 2A). To test

the binding of GAL3 protein to its channel, GAL3 protein (0.25 μg/well) was coated on a plate. Various concentrations of biotinylated GAL3 binding peptide, channel, or anti-GAL3 antibody were added to well. Background binding to no protein wells was subtracted out. The ELISA results suggested that GAL3 protein can bind to GAL3 channel with high efficiency, but not to control EpCAM channel (Fig. 2B). The GAL3 protein could also bind to GAL3 peptide and antibody (Fig. 2B).

Real-time sensing of GAL3 protein and TF-HSA complex interaction with engineered phi29 connector channels

Under a 0.15 M KCl, 5 mM HEPES, pH 7.4 buffer solution, the binding events (Fig. 3A) with a long dwell time and a signature shape of a rectangle were observed, representing specific and tight binding between the probe on the connector and the GAL3 protein. Notably, these rectangular-like signals share a common characteristic in that the specific binding events occur with roughly a 32 % current blockage and long dwell time permitting them to be a reliable signature for clinical sample detection. The GAL3 (antigen) binding to its specific probe (like-antibody) will result in conformation changes of the connector. Conformational changes are described as a decreasing 30 % three-step even resulting in a near closing of the pore, which can be induced by high voltage or by affinity binding on the C-terminal.[47] Here, the current blockage percentage was calculated, and a ~31 % blockage was observed (Fig. 3B). The GAL3 binding events could also be distinguished from nonspecific noise by the result of forming a scatter plot of dwell time versus current blockage (Fig. 3C). Similar results were obtained when the N-His-GP10-TF channel was exposed to the TF-HSA complex (Fig. 3D-F). Interestingly, two-steps current blockage events were also observed in N-His-GP10-TF channel, meaning that two TF-HSA complex simultaneously bound to the connector (Fig. 3D, green color).

Real-time sensing of free TF antigen interaction with engineered phi29 connector channels

Since TF-HSA complex could specifically bind to TF channel, we then tested the binding of free TF to the TF channel. The insertion of the TF engineered connector channels generated a stepwise increase of the current, as shown in the continuous current trace (Fig. 4A). The open channel is about 55pA after one channel insertion in 0.2 M KCl, 5 mM HEPES, pH 7.4 buffer. Robust binding signals appeared immediately after the second channel insertion. The binding of the free TF (50 μg/ml) to each probe induced stepwise blocks (every block represented a single molecule binding) in current (Fig. 4A and B). The specific binding capability of free TF antigen to channel is also proved by the histograms of the current blockage result (Fig. 4C) and scatter plot result (Fig. 4D). TF is a carbohydrate antigen, we tested sucrose and BSA as control, no binding signal was observed (data not shown).

Selectivity of the GAL3 probe for GAL3 protein in the presence of protein impurities

To confirm the current blockage was not caused by the translocation of tumor biomarker protein through the channel, a standard control protein (Carbonic Anhydrase, CA) with the same molecular weight (29 kDa) was adopted to measure the current blockage (Fig. 5). As shown in Fig. 5A, there are no binding events occurring with enough frequency to be considered above background noise levels. The current blockage and scatter plot results also confirmed this result (Fig. 5B and C). However, under the same buffer conditions containing

the CA protein, we then added the GAL3 protein into both chambers. The specific binding events with a long dwell time and rectangular signature shape appeared (Fig. 5D). We noted another event grouping, centered current blockage at about 33 % (Fig. 5E). This new event group's position was consistent with the previous blockage distribution of GAL3 protein using the same buffer without nonspecific protein, indicating that this new group was caused by GAL3 protein interaction with the probe. The scattering of dwell time versus current blockage results also confirmed this result (Fig. 5F).

Breast cancer biomarker detection from patient NAF samples using engineered phi29 connector

One of the challenges of real-time detecting for specific tumor markers in NAF samples is the extremely low abundance (e.g. TF 0–2240 ng/ul)[14] of the target protein and complex interfering proteins. Here, our results showed a label-free, amplification-free, real-time, and rapid detection method by using an engineered phi29 GP10 connector. In testing these samples, the fluids are further diluted (1:600) in the nanopore system thereby making the amount of biomarkers even sparser; however, our system has reliably detected these samples repeatedly. The specific binding signal can be distinguished with 100 % accuracy from the background and non-specific binding signals by longer dwell time, current blockage percentage (about 32 %), and signature shape (rectangular minaret-like) (Fig. 6B and E). When the breast cancer NAF samples were added to both chambers, another permanent binding signal with a longer dwell time (~0.07 s) was also observed, representing much more tight binding between the probe on the connector and the biomarker antigen in NAF samples. Excitingly, the biomarkers of the breast cancer NAF sample show significantly higher binding numbers than those from the healthy one $(p < 0.05)$, which means the biomarker in the breast cancer NAF sample was in higher abundance than the normal samples (Fig. 6C and F). To prove the signal is the interaction of the biomarker in the NAF with the corresponding channel, the breast cancer NAF sample was also tested on the N-his-GP10-EpCAM probe, which was designed for testing EpCAM antibody. When the NAF samples from breast cancer patients were added to the N-his-GP10-EpCAM channel, long-term observation results show no specific signal appearing (Data not shown). The current trace results without NAF samples were used as the control (Fig. 6A and D).

Discussion

Breast cancer is the most common cancer among females in the world. Early-stage cancer detection could reduce breast cancer death rates significantly in the long-term[48]. To reduce morbidity and mortality, more sensitive methods for early diagnosis of breast cancer are warranted. The cancer secretome (secreted antigens and metabolites) represents a very promising approach to detect cancer-related biomarkers directly in body fluids mirroring the tissue-specific tumor microenvironment. NAF for breast cancer that is secreted by non-pregnant women[6]. The NAF secreted by epithelial and stromal cells lining the breast duct can be collected from patients in a painless, non-invasive out-patient clinical setting using breast pumps. However, inflammatory breast cancer is often confused with mastitis that is caused by microbial infection of the breast. The clinical symptoms of inflammatory breast cancer are very similar to that of mastitis. Currently, differential diagnosis between

inflammatory breast cancer and mastitis via nipple aspirate fluid is also challenging. The NAF secretome, with its rich repertoire of candidate biomarkers some of which are unique to cancer cells, represents an excellent opportunity for early diagnosis of breast cancer, limiting the decreased tumor-specificity of surrogate breast cancer biomarkers circulating in the blood[49,50]. ELISA is one of the most specific and straightforward assays for detecting biomolecules in research and clinics. With the development of the high-throughput device, different types of ELISA are now available to detect various biomarkers at the high-throughput level. However, the ELISA technique has distinct disadvantages, that is the limited detection threshold, expensive and time-consuming, and sensitivity. Importantly, ELISA assay always requires a larger sample volume. This is inappropriate for precious and difficult-to-obtain samples. Nanopore single molecule detection technology overcomes this shortcoming. As a new sensing technology, it has the advantages of no labeling, single molecule detection, high sensitivity, fast detection speed, real-time monitoring, and simple operation. It is widely used in gene sequencing, the detection of peptides and proteins, markers and microorganisms, and other biomolecules and metal ions. To overcome the throughput issue, Oxford Nanopore has developed an ultra-high throughput desktop nanopores device for molecular analyses.

Glycoantigens are potential biomarkers for breast cancer assessment[14]. Epithelial cancer cells exhibit increased cell surface expression of mucin-type antigens with aberrant O-glycosylation. Among such antigens, TF is displayed on cell surface proteins and lipids in ~90 % of breast adenocarcinomas[44,51]. At the same time, TF can mobilize GAL3 secretion from epithelial cells[52]. Galectin-3, a member of the β-galactoside-binding lectin family, is involved in several biological events and could be served as a useful diagnostic biomarker. GAL3, as an oncological biomarker, plays an important role in breast cancer tumors because of its ability to promote interactions between cell-cell and cell-extracellular matrix (ECM) elements, increasing tumor survival and metastatic dissemination[53].

Phage Peptide Display (PPD) is a powerful research tool for high-throughput screening of protein interactions. It can be used to select bioactive peptides bound to receptors or proteins[54]. PPD is a selection technique in which a peptide or protein is fused with a bacteriophage coat protein and displayed on the surface of a virion. Utilizing novel combinatorial phage display approaches, Deutscher et al., have generated a series of peptides targeting breast cancer-associated antigens, including PPDs that bind Gal-3 and TF[17,45,55].

Here the breast cancer biomarker detection platform is based on stepwise conformational changes of the channel induced by binding of ligands to probes immobilized on the connector. We discovered that the DNA packaging motors' of bacteriophages SPP1, T3, T4, and phi29 all exercise three discrete steps of gating (shrinking) during DNA translocation, with each step reducing 32 % of channel dimensions[40]. These three-step conformational changes of phi29 GP10 connector could be induced by a higher voltage (>100 mV) or by affinity binding to the C-terminal wider end located within the capsid[47].

Conclusion

We developed a simple, sensitive, and robust single pore diagnostic platform based on a biological motor's elegant and elaborate protein channel for the detection of breast cancer biomarkers from breast cancer patient NAF with high sensitivity and specificity. This platform enables breast cancer diagnosis at early stages, thus leading to a more treatable diagnosis. This platform can easily be translated into a high-throughput multiplexed biomarker quantification tool for diagnosing many diseases.

Acknowledgement

The research of NAF and breast cancer diagnosis was supported by NIH grant R01EB012135 (to P.G.). The research on nanopore sensing was partial supported by a Sponsor Research Contract from Oxford Nanopore Technologies Ltd. to The Ohio State University (to P.G.). We thank all the volunteers who provided NAF samples for studies on early breast cancer diagnosis.

References

1. Heywang-Kobrunner SH, Hacker A, Sedlacek S. Advantages and disadvantages of mammography screening. Breast Care (Basel) 2011;6(3):199–207. [PubMed: 21779225]
2. Petrakis NL. Nipple aspirate fluid in epidemiologic studies of breast disease. Epidemiol Rev 1993;15(1):188–95. [PubMed: 8405203]
3. Fabian CJ, Kimler BF, Mayo MS, Khan SA. Breast-tissue sampling for risk assessment and prevention. Endocr Relat Cancer 2005;12(2):185–213. [PubMed: 15947097]
4. Kouriefs C, Leris AC, Mokbel K. Nipple aspirate fluid in relation to breast cancer. Breast 2000;9(2):113.
5. Sauter ER, Ross E, Daly M, Klein-Szanto A, Engstrom PF, Sorling A, et al. Nipple aspirate fluid: a promising non-invasive method to identify cellular markers of breast cancer risk. Br J Cancer 1997;76(4):494–501. [PubMed: 9275027]
6. Schaaij-Visser TB, de Wit M, Lam SW, Jimenez CR. The cancer secretome, current status and opportunities in the lung, breast and colorectal cancer context. Biochim Biophys Acta 2013;1834(11):2242–58. [PubMed: 23376433]
7. Sauter ER. Analysis of nipple aspirate fluid for diagnosis of breast cancer: an alternative to invasive biopsy. Expert Rev Mol Diagn 2005;5(6):873–81. [PubMed: 16255629]
8. Qin W, Gui G, Zhang K, Twelves D, Kliethermes B, Sauter ER. Proteins and carbohydrates in nipple aspirate fluid predict the presence of atypia and cancer in women requiring diagnostic breast biopsy. BMC Cancer 2012;12:52. [PubMed: 22296682]
9. Sauter ER, Zhu W, Fan XJ, Wassell RP, Chervoneva I, Du Bois GC. Proteomic analysis of nipple aspirate fluid to detect biologic markers of breast cancer. Br J Cancer 2002;86(9):1440–3. [PubMed: 11986778]
10. Henderson G, Ulsemer P, Schober U, Loffler A, Alpert CA, Zimmermann-Kordmann M, et al. Occurrence of the human tumor-specific antigen structure Galbeta1-3GalNAcalpha- (Thomsen-Friedenreich) and related structures on gut bacteria: prevalence, immunochemical analysis and structural confirmation. Glycobiology 2011;21(10):1277–89. [PubMed: 21551457]
11. Farhad M, Rolig AS, Redmond WL. The role of Galectin-3 in modulating tumor growth and immunosuppression within the tumor microenvironment. Oncoimmunology 2018;7(6)e1434467. [PubMed: 29872573]
12. Wang Y, Liu S, Tian Y, Wang Y, Zhang Q, Zhou X, et al. Prognostic role of galectin-3 expression in patients with solid tumors: a meta-analysis of 36 eligible studies. Cancer Cell Int 2018;18:172. [PubMed: 30410421]
13. Deutscher SL, Dickerson M, Gui G, Newton J, Holm JE, Vogeltanz-Holm N, et al. Carbohydrate antigens in nipple aspirate fluid predict the presence of atypia and cancer in women requiring diagnostic breast biopsy. BMC Cancer 2010;10:519. [PubMed: 20920311]

14. Kumar SR, Sauter ER, Quinn TP, Deutscher SL. Thomsen-friedenreich and tn antigens in nipple fluid: carbohydrate biomarkers for breast cancer detection. Clin Cancer Res 2005;11(19 Pt 1):6868–71. [PubMed: 16203776]
15. Shaheed SU, Tait C, Kyriacou K, Linforth R, Salhab M, Sutton C. Evaluation of nipple aspirate fluid as a diagnostic tool for early detection of breast cancer. Clin Proteomics 2018;15:3. [PubMed: 29344009]
16. Shaheed SU, Tait C, Kyriacou K, Mullarkey J, Burrill W, Patterson LH, et al. Nipple aspirate fluid-a liquid biopsy for diagnosing breast health. Proteomics Clin Appl 2017(9–10):11.
17. Kumar SR, Gallazzi FA, Quinn TP, Deutscher SL. (64)Cu-labeled peptide for PET of breast carcinomas expressing the thomsen-friedenreich carbohydrate antigen. J Nucl Med 2011;52(11):1819–26. [PubMed: 21984800]
18. Li J, Guan X, Fan Z, Ching LM, Li Y, Wang X. Non-invasive biomarkers for early detection of breast cancer. Cancers (Basel) 2020;12(10).
19. Twelves D, Nerurkar A, Osin P, Ward A, Isacke CM, Gui GP. The feasibility of nipple aspiration and duct lavage to evaluate the breast duct epithelium of women with increased breast cancer risk. Eur J Cancer 2013;49(1):65–71. [PubMed: 22921156]
20. Kuerer HM, Goldknopf IL, Fritsche H, Krishnamurthy S, Sheta EA, Hunt KK. Identification of distinct protein expression patterns in bilateral matched pair breast ductal fluid specimens from women with unilateral invasive breast carcinoma. High-throughput biomarker discovery. Cancer 2002;95(11):2276–82. [PubMed: 12436432]
21. Pawlik TM, Hawke DH, Liu Y, Krishnamurthy S, Fritsche H, Hunt KK, et al. Proteomic analysis of nipple aspirate fluid from women with early-stage breast cancer using isotope-coded affinity tags and tandem mass spectrometry reveals differential expression of vitamin D binding protein. BMC Cancer 2006;6:68. [PubMed: 16542425]
22. Tessitore A, Gaggiano A, Cicciarelli G, Verzella D, Capece D, Fischietti M, et al. Serum biomarkers identification by mass spectrometry in high-mortality tumors. Int J Proteomics 2013;2013125858. [PubMed: 23401773]
23. Macklin A, Khan S, Kislinger T. Recent advances in mass spectrometry based clinical proteomics: applications to cancer research. Clin Proteomics 2020;17:17. [PubMed: 32489335]
24. Petrera A, von Toerne C, Behler J, Huth C, Thorand B, Hilgendorff A, et al. Multiplatform approach for plasma proteomics: complementarity of olink proximity extension assay technology to mass spectrometry-based protein profiling. J Proteome Res 2021;20(1):751–62. [PubMed: 33253581]
25. Kondo T. Cancer biomarker development and two-dimensional difference gel electrophoresis (2D-DIGE). Biochim Biophys Acta Proteins Proteom 2019;1867(1):2–8. [PubMed: 30392560]
26. Meleady P. Two-dimensional gel electrophoresis and 2D-DIGE. Methods Mol Biol 2018;1664:3–14. [PubMed: 29019120]
27. Chandramouli K, Qian PY. Proteomics: challenges, techniques and possibilities to overcome biological sample complexity. Hum Genomics Proteomics 2009;2009.
28. Deyati A, Younesi E, Hofmann-Apitius M, Novac N. Challenges and opportunities for oncology biomarker discovery. Drug Discov Today 2013;18(13–14):614–24. [PubMed: 23280501]
29. Branton D, Deamer DW, Marziali A, Bayley H, Benner SA, Butler T, et al. The potential and challenges of nanopore sequencing. Nat Biotechnol 2008;26(10):1146–53. [PubMed: 18846088]
30. Venkatesan BM, Bashir R. Nanopore sensors for nucleic acid analysis. Nat Nanotechnol 2011;6(10):615–24. [PubMed: 21926981]
31. Majd S, Yusko EC, Billeh YN, Macrae MX, Yang J, Mayer M. Applications of biological pores in nanomedicine, sensing, and nanoelectronics. Curr Opin Biotechnol 2010;21(4):439–76. [PubMed: 20561776]
32. Haque F, Geng J, Montemagno C, Guo P. Incorporation of a viral DNA-packaging motor channel in lipid bilayers for real-time, single-molecule sensing of chemicals and double-stranded DNA. Nat Protoc 2013;8(2):373–92. [PubMed: 23348364]
33. Simpson AA, Leiman PG, Tao Y, He Y, Badasso MO, Jardine PJ, et al. Structure determination of the head-tail connector of bacteriophage phi29. Acta Crystallogr D Biol Crystallogr 2001;57(Pt 9):1260–9. [PubMed: 11526317]

34. Simpson AA, Tao Y, Leiman PG, Badasso MO, He Y, Jardine PJ, et al. Structure of the bacteriophage phi29 DNA packaging motor. Nature 2000;408(6813):745–50. [PubMed: 11130079]
35. Zhang L, Gardner ML, Jayasinghe L, Jordan M, Aldana J, Burns N, et al. Detection of single peptide with only one amino acid modification via electronic fingerprinting using reengineered durable channel of Phi29 DNA packaging motor. Biomaterials 2021;276121022.
36. Haque F, Wang S, Stites C, Chen L, Wang C, Guo P. Single pore translocation of folded, double-stranded, and tetra-stranded DNA through channel of bacteriophage phi29 DNA packaging motor. Biomaterials 2015;53:744–52. [PubMed: 25890769]
37. Geng J, Wang S, Fang H, Guo P. Channel size conversion of Phi29 DNA-packaging nanomotor for discrimination of single- and double-stranded nucleic acids. ACS Nano 2013;7(4):3315–23. [PubMed: 23488809]
38. Haque F, Lunn J, Fang H, Smithrud D, Guo P. Real-time sensing and discrimination of single chemicals using the channel of phi29 DNA packaging nanomotor. ACS Nano 2012;6(4):3251–61. [PubMed: 22458779]
39. Wang S, Haque F, Rychahou PG, Evers BM, Guo P. Engineered nanopore of Phi29 DNA-packaging motor for real-time detection of single colon cancer specific antibody in serum. ACS Nano 2013;7(11):9814–22. [PubMed: 24152066]
40. Wang S, Ji Z, Yan E, Haque F, Guo P. Three-step channel conformational changes common to DNA packaging motors of bacterial viruses T3, T4, SPP1, and Phi29. Virology 2017;500:285–91. [PubMed: 27181501]
41. Ji Z, Guo P. Channel from bacterial virus T7 DNA packaging motor for the differentiation of peptides composed of a mixture of acidic and basic amino acids. Biomaterials 2019;214119222.
42. Ji Z, Kang X, Wang S, Guo P. Nano-channel of viral DNA packaging motor as single pore to differentiate peptides with single amino acid difference. Biomaterials 2018;182:227–33. [PubMed: 30138785]
43. Keser T, Tijardovic M, Gornik I, Lukic E, Lauc G, Gornik O, et al. High-throughput and site-specific N-glycosylation analysis of human alpha-1-acid glycoprotein offers a great potential for new biomarker discovery. Mol Cell Proteomics 2020;20100044.
44. Glinsky VV, Glinsky GV, Rittenhouse-Olson K, Huflejt ME, Glinskii OV, Deutscher SL, et al. The role of thomsen-friedenreich antigen in adhesion of human breast and prostate cancer cells to the endothelium. Cancer Res 2001;61(12):4851–7. [PubMed: 11406562]
45. Kumar SR, Deutscher SL. 111In-labeled galectin-3-targeting peptide as a SPECT agent for imaging breast tumors. J Nucl Med 2008;49(5):796–803. [PubMed: 18413389]
46. Glinsky VV, Huflejt ME, Glinsky GV, Deutscher SL, Quinn TP. Effects of thomsen-friedenreich antigen-specific peptide P-30 on beta-galactoside-mediated homotypic aggregation and adhesion to the endothelium ofMDA-MB-435 human breast carcinoma cells. Cancer Res 2000;60(10):2584–8. [PubMed: 10825125]
47. Geng J, Fang H, Haque F, Zhang L, Guo P. Three reversible and controllable discrete steps of channel gating of a viral DNA packaging motor. Biomaterials 2011;32(32):8234–42. [PubMed: 21807410]
48. Migowski A. Early detection of breast cancer and the interpretation of results of survival studies. Cien Saude Colet 2015;20(4):1309. [PubMed: 25923642]
49. Varnum SM, Covington CC, Woodbury RL, Petritis K, Kangas LJ, Abdullah MS, et al. Proteomic characterization of nipple aspirate fluid: identification of potential biomarkers of breast cancer. Breast Cancer Res Treat 2003;80(1):87–97. [PubMed: 12889602]
50. He J, Gornbein J, Shen D, Lu M, Rovai LE, Shau H, et al. Detection of breast cancer biomarkers in nipple aspirate fluid by SELDI-TOF and their identification by combined liquid chromatography-tandem mass spectrometry. Int J Oncol 2007;30(1):145–54. [PubMed: 17143523]
51. Springer GF. T and tn, general carcinoma autoantigens. Science 1984; 224(4654):1198–206. [PubMed: 6729450]
52. Glinsky VV, Glinsky GV, Glinskii OV, Huxley VH, Turk JR, Mossine VV, et al. Intravascular metastatic cancer cell homotypic aggregation at the sites of primary attachment to the endothelium. Cancer Res 2003;63(13):3805–11. [PubMed: 12839977]

53. Liu FT, Rabinovich GA. Galectins as modulators of tumour progression. Nat Rev Cancer 2005;5(1):29–41. [PubMed: 15630413]

54. Wu CH, Liu IJ, Lu RM, Wu HC. Advancement and applications of peptide phage display technology in biomedical science. J Biomed Sci 2016;23:8. [PubMed: 26786672]

55. Hansen M, Wind T, Blouse GE, Christensen A, Petersen HH, Kjelgaard S, et al. A urokinase-type plasminogen activator-inhibiting cyclic peptide with an unusual P2 residue and an extended protease binding surface demonstrates new modalities for enzyme inhibition. J Biol Chem 2005; 280(46):38424–37. [PubMed: 16141208]

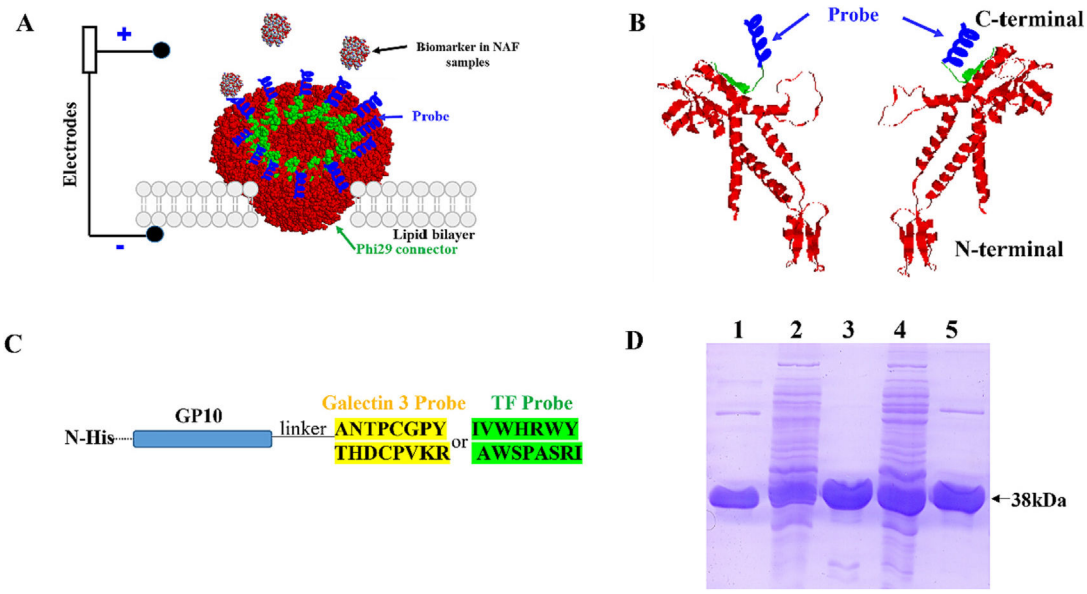

Fig. 1.

Illustration and characterization of the channel of engineered phi29 bacterial virus DNA packaging motor. (A) Schematic diagram of real-time detection breast cancer biomarkers from clinic NAF samples. (B) Cross-section structure of the GP 10 connector showing the location of the probe (blue); (C) Construction of the modified gp10 gene by insertion of His tag at the N-terminus, 2-Gly linker and GAL3 or TF probe at the C-terminus; (D) Molecular weight of purified N-His-GP10-GAL3 protein (lane 1,38 kDa), unpurified N-His-GP10-GAL3 protein (lane 2), purified N-His-GP10-TF protein (lane 3,38 kDa), unpurified N-His-GP10-TF protein (lane 4), and control GP10 protein(lane 5) on 10 % SDS-PAGE.

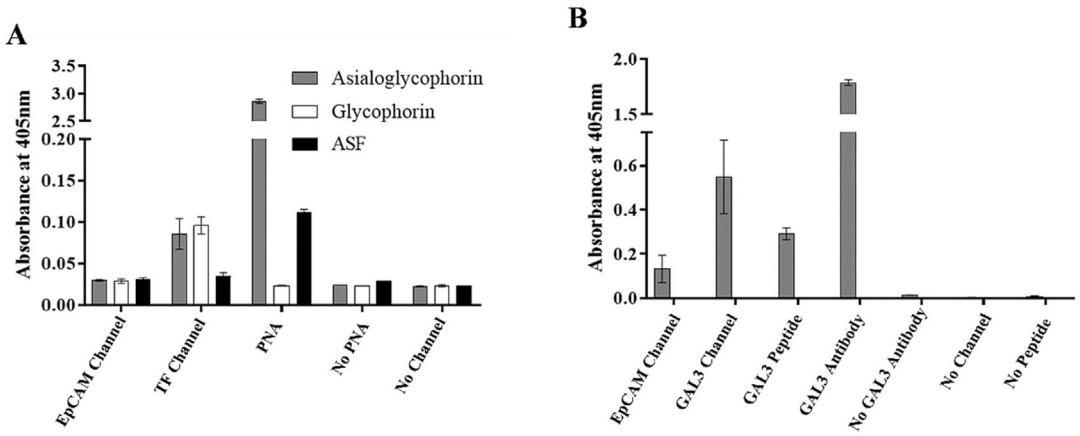

Fig. 2.

Evaluation of biomarkers binding to the motor by ELISA. (A) Asialoglycophorin, glycophorin, asialofetuin or no protein were coated on a plate o/n at 4 °C. After washing, TF channel or biotinylated PNA (BPNA) were added and incubated in an appropriate secondary antibody. Plates were read at 405 nm. (B) GAL3 protein was coated on a plate and various concentrations of biotinylated peptide, channel, or anti-GAL3 antibody were added to well to test the binding efficiency. SA-HRP, anti-HisAb-HRP or antiRat-HRP were used as secondary antibodies. Plates were read at 405 nm.

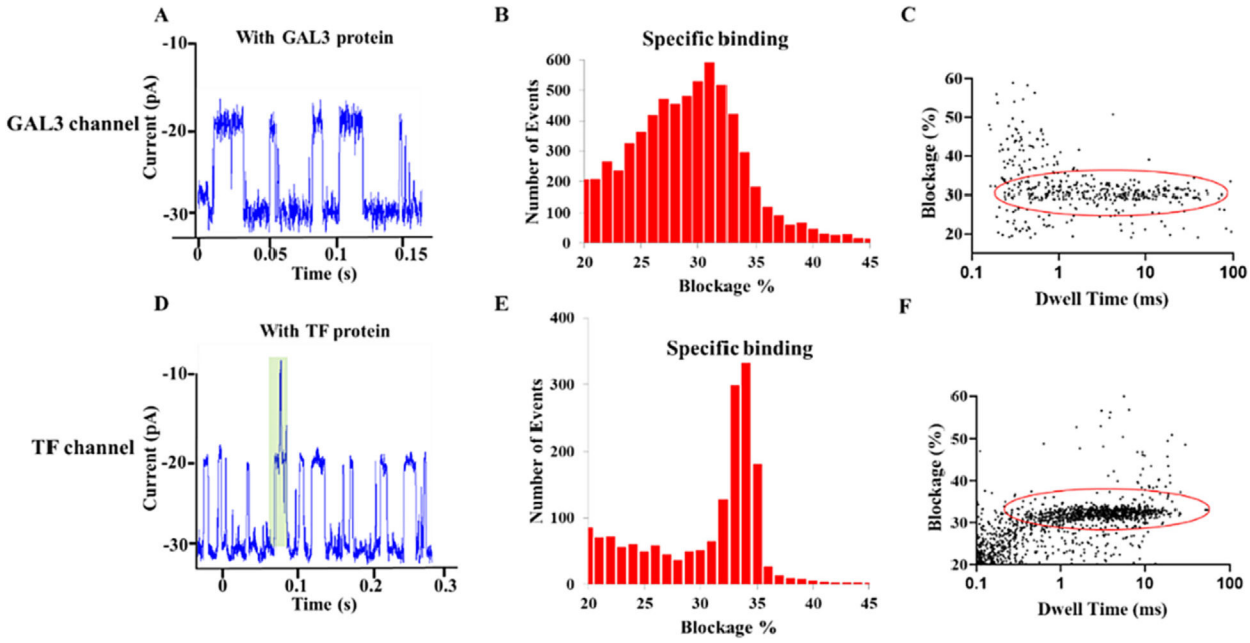

Fig. 3.

Real-time sensing of cancer biomarkers interaction with engineered phi29 connector channels: (A, D) Current trace results after the addition of the GAL3 protein (A) or TF-HSA (D) antigen. (B, E) Histograms of current blockage after the addition of antigen to corresponding channels; (C, F) Scatter of dwell time versus current blockage result after the addition of GAL3 protein (C) or TF-HSA (F) complex to corresponding channels.

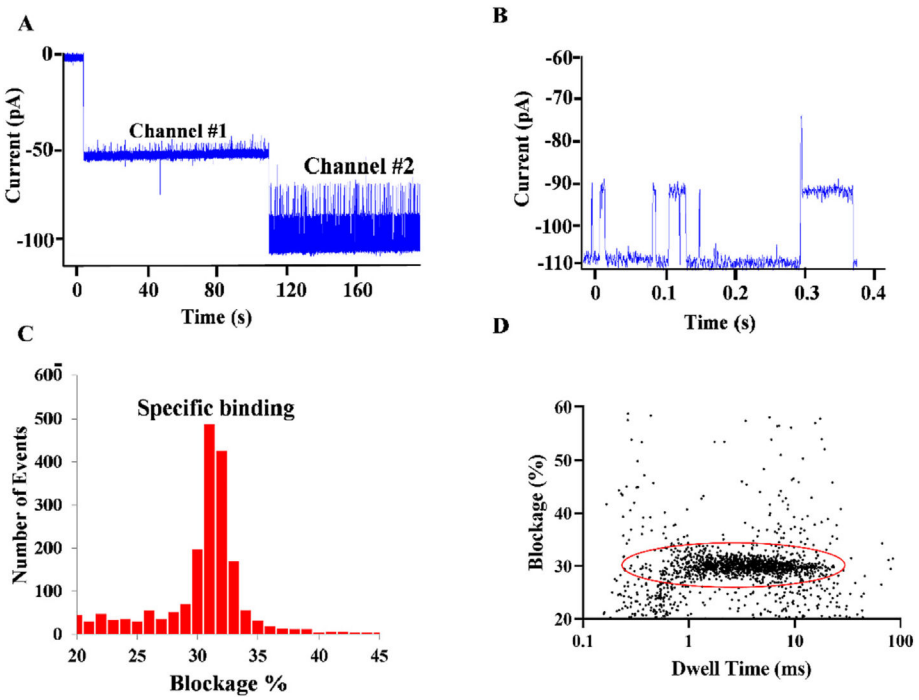

Fig. 4.

Free TF antigen bind to engineered phi29 connector channels: (A) Continuous current trace showing two insertions of TF reengineered connector channels into planar lipid bilayer and the appearance of the signal after the second chamber insertion. (B) Representative current trace result from (A). (C) Histograms of current blockage after the addition of free TF antigen to channel. (D) Scatter of dwell time versus current blockage result after the addition of free TF antigen.

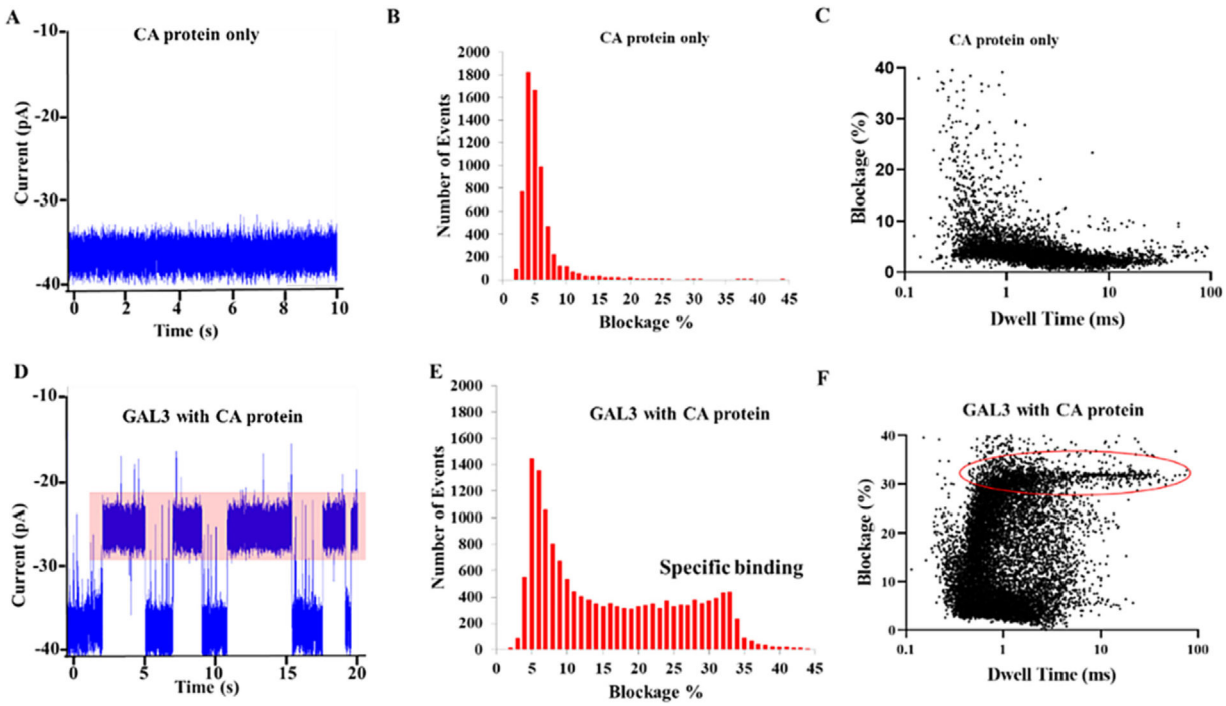

Fig. 5.

GAL3 protein detection in the presence of nonspecific control CA protein with same MW: (A) After addition of CA protein; (B) Histograms of current blockage after the addition of CA protein; (C) Scatter of dwell time versus current blockage after addition of CA protein; (D) Specific GAL3 protein binding events in the presence of CA protein; (E) Histograms of current blockage after the addition of GAL3 protein in the presence of CA protein; (F) Scatter of dwell time versus current blockage after addition of GAL3 protein in the presence of CA protein.

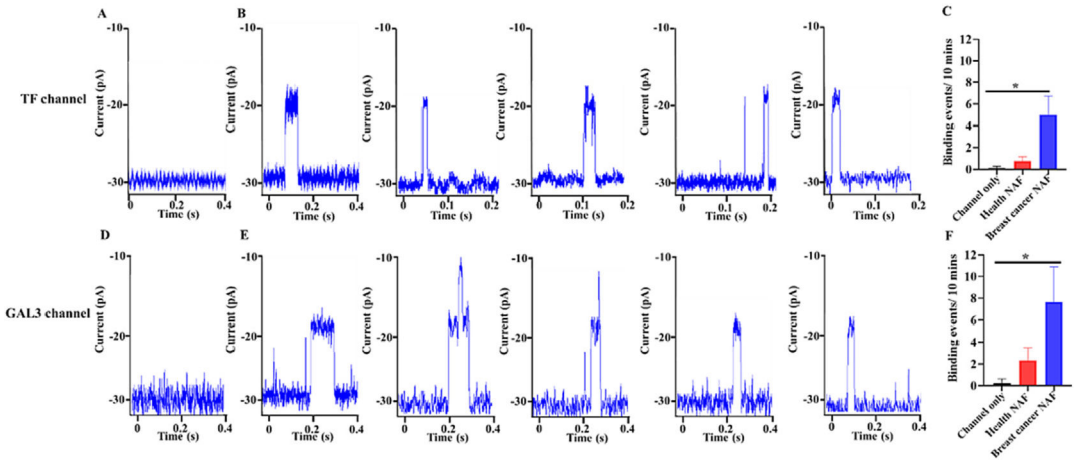

Fig. 6.

Breast cancer biomarker detection from the health and breast cancer patient NAF samples using engineered phi29 connector. (A, B) Current trace results showing representative specific binding events before (A) and after (B) the addition of NAF samples from breast cancer patients to the TF channel. (D, E) Current trace results showing representative specific binding events before (D) and after (E) the addition of NAF samples from breast cancer patients to the GAL3 channel. (C, D) Statistical results of specific binding events from health NAF samples or breast cancer NAF samples in 10 min on N-his-GP10-TF channel (C) and N-his-GP10-GAL3 channel (D). *$p < 0.05$.

Table 1

Clinical data for NAF collection.

Date of collection	De-identification Number Left Breast (NASL)	De-identification Number Right Breast (NASR)	Clinical Notes	Age	Tumor information
12/15/2020	NAF-1L	NAF-1R	Bilateral breast cancer; T1cN0M0, stage IA	65 yrs., female	Left: Stage IIIA, 8.3 cm, Ductal histology, ER+, PR+, HER2− Right: Stage IA, 2.9 cm, Ductal, ER+, PR+, HER2−.
06/08/2021	NAF-2L	NAF-2R	Tumor was in left breast	52 yrs., female	Left: Stage IA, 0.8 cm, Ductal, ER+, PR+, HER2−.